Bull. Mater. Sci., Vol. 23, No. 5, October 2000, pp. 399–403. © Indian Academy of Sciences.

Corrosion of carbon-alloyed iron aluminides

M SEN, R BALASUBRAMANIAM* and A V RAMESH KUMAR†

Department of Materials and Metallurgical Engineering, Indian Institute of Technology, Kanpur 208 016, India
†Defence Materials Stores and Research Development Establishment, Kanpur 208 013, India

MS received 22 May 2000; revised 17 August 2000

Abstract. The corrosion behaviour of two carbon-alloyed intermetallics of composition Fe–28·1Al–2·1C and Fe–27·5Al–3·7C has been studied and compared with that of binary intermetallics. Potentiodynamic polarization studies indicated that the intermetallics exhibited active–passive behaviour in an acidic solution of pH = 1, whereas they exhibited stable passivity in a buffer solution of pH 8·4. Corrosion rates were also obtained by immersion testing. The variation of corrosion rate as a function of time was similar for both the intermetallics. The variation in corrosion rate as a function of time has been explained based on the observed potentiodynamic polarization behaviour. Scanning electron microscopy of corroded surfaces indicated that the carbon-alloyed intermetallics were susceptible to galvanic corrosion, due to the presence of carbides.

Keywords. Corrosion; iron aluminides; Fe_3Al; potentiodynamic polarization.

1. Introduction

Ordered intermetallic alloys based on iron aluminides of composition Fe_3Al and FeAl are being considered for high temperature structural applications. Although these alloys exhibit poor room temperature ductility and low fracture toughness, significant improvement in these respects can be achieved by alloying additions and process control. Most of the available literature deals with iron aluminide compositions with very low (< 0·01 wt%) carbon contents because carbon causes significant reduction in ductility. Recently, Baligdad *et al* (1997a) reported that addition of carbon in the range of 0·14 to 0·50 wt% significantly increased the room temperature strength of Fe–16 wt% (28 at%) Al alloys. These alloys also exhibited relatively significant room temperature ductilities, which was attributed to irreversible trapping of hydrogen at Fe_3AlC carbide–matrix interfaces (Baligdad *et al* 1997b). The trapping of hydrogen at these interfaces has been confirmed by hydrogen diffusivity measurements in carbon-alloyed iron aluminides (Sen and Balasubramaniam 2000). Moreover, the carbon-alloyed iron aluminides were stronger and this increase in room temperature yield strength was attributed to solid solution strengthening by the interstitial carbon, as well as precipitation hardening due to the presence of Fe_3AlC precipitates (Baligdad *et al* 1997b). The aim of the present study is to understand the ambient temperature corrosion behaviour of these intermetallics.

*Author for correspondence

2. Experimental

The carbon-alloyed iron aluminides were obtained in the form of rolled metal strips (Baligdad *et al* 1994) from the Defence Metallurgical Research Laboratory, Hyderabad. Their composition (in at%) were Fe–28·1Al–2·1C and Fe–27·5Al–3·7C. In order to understand the polarization behaviour of these intermetallics, square sections of 1 cm side, were sectioned and connected to a conductive wire. The specimens were mounted in a cold-setting epoxy. The specimen surfaces were polished to 600 grit surface finish and were properly cleaned with acetone prior to polarization experiments. Polarization experiments were performed in an electrochemical polarization cell using a potentiostat (EG & G 273 model) interfaced to a personal computer. A platinum foil of 1 cm^2 area was used as the counter electrode. A 0·05 mol/l H_2SO_4 solution of pH = 1, and a buffer solution (0·15 N H_3BO_3 + 0·15 N $Na_2B_4O_7$–$10H_2O$) of pH = 8·44 were the electrolytes used in the present study. Before each polarization experiment, the specimen was immersed in the electrolyte and the free corrosion potential (FCP) was monitored as a function of time. The potential was monitored continuously using standard calomel electrode (SCE) attached to the luggin capillary. All potentials referred in this paper are with respect to SCE. The FCP stabilized usually in a short time. Once the steady state FCP were obtained, the potentiodynamic polarization experiment was performed at a scan rate of 1 mV/sec. The potential was scanned from active to noble direction. The temperature of the polarization cell was not controlled and all experiments were performed at ambient temperature (25°C).

The corrosion rates of the alloys were also determined in the 0·05 mol/l H_2SO_4 solution by constant immersion testing. Two types of immersion tests were performed. The first type was a relatively long term testing for a total period of 8 days with weight losses being measured after every 12 h. In the second type, experiments were performed for a total duration of only 24 h with weight losses measured at 30 min intervals. The weight loss data previously obtained by Babu *et al* (2000) for Fe–25Al and Fe–28 Al intermetallics in the same solution have been compared.

3. Results and discussion

3.1 *Potentiodynamic polarization*

The potentiodynamic polarization curves obtained in the acidic medium for the carbon-alloyed intermetallics, along with that for the Fe–28Al intermetallic, are presented in figure 1, while the results obtained in the buffer solution are presented in figure 2. Both the carbon-alloyed intermetallics exhibited active–passive behaviour in the acidic solution, in that there was a region where the current density was lowered on polarizing past the zero current potential. The passivity parameters from these plots are tabulated in table 1. In the buffer solution, the nature of the polarization curves indicated that both the carbon-alloyed intermetallics passivated readily on immersion. The passive current densities (i_{pass}) for both the intermetallics were lower in the buffer solution, when compared to those in the acidic solution.

In the acidic solution, the critical current density for passivation (i_{crit}) was lower for Fe–28·1Al–2·1C when compared to Fe–27·5Al–3·7C. Moreover, the i_{crit} for the binary Fe–28Al was lower than those of both these intermetallics, thereby indicating that the i_{crit} increased with increasing carbon addition. As regards the passive region in the 0·05 mol/l H_2SO_4 solution, for the Fe–28Al intermetallic (without carbon addition), the passive current density (i_{pass}) was equal to $7{\cdot}4 \times 10^{-5}$ A/cm^2 and the potential for primary passivation (E_{pass}) was 0·37 V (Babu *et al* 2000). In the same solution, the measured i_{pass} were $8{\cdot}3 \times 10^{-5}$ A/cm^2 and $7{\cdot}2 \times 10^{-5}$ A/cm^2 for Fe–28·1Al–2·1C and Fe–27·5Al–3·7C, respectively. Moreover, the E_{pass} were 0·36 V and 0·41 V for Fe–28·1Al–2·1C and Fe–27·5Al–3·7C, respectively.

The corrosion rates were determined from the active region of the polarization curves (obtained in the acidic

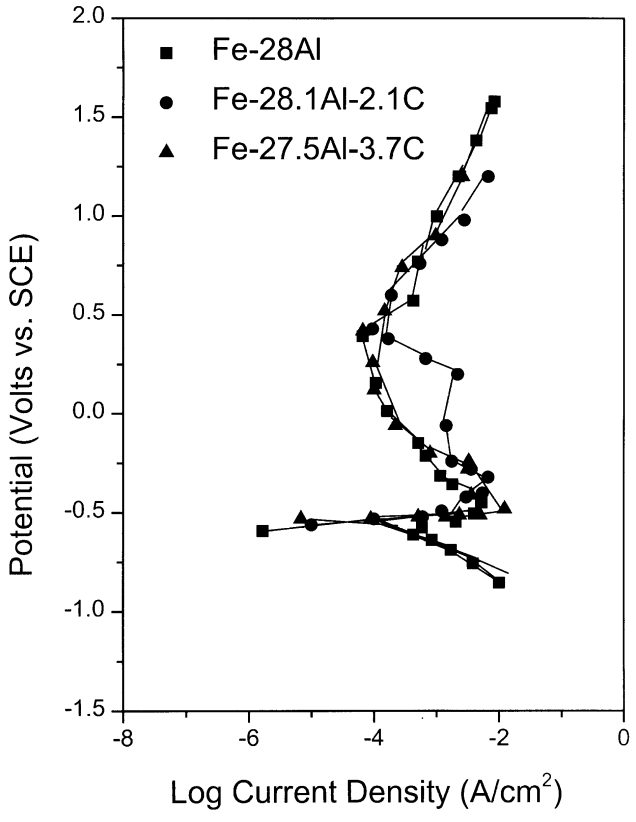

Figure 1. Potentiodynamic polarization diagrams obtained in 0·05 mol/l H_2SO_4 solution of pH = 1, at a scan rate of 1 mV/s. The intermetallics exhibited active–passive behaviour. The data for Fe–28Al is from Babu *et al* (2000).

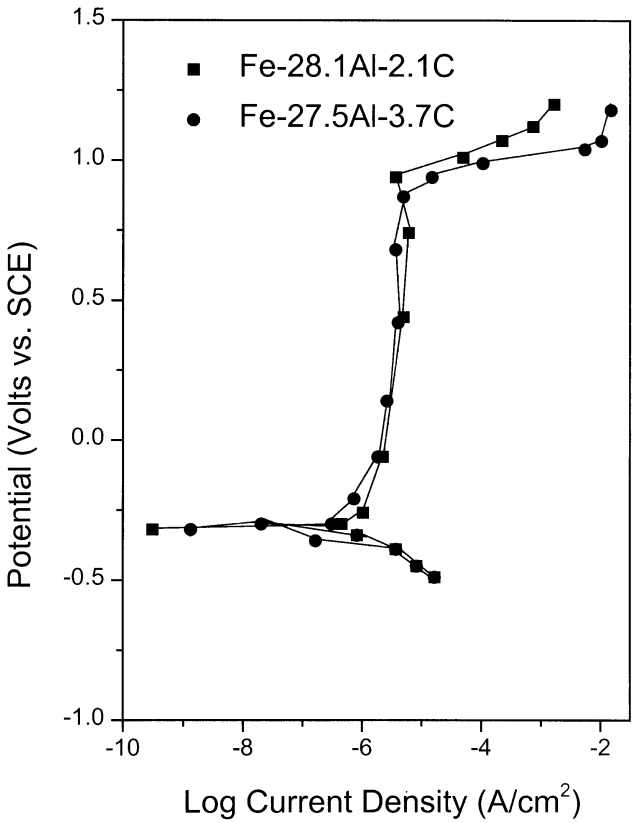

Figure 2. Potentiodynamic polarization diagrams obtained in 0·15 N H_3BO_3 + 0·15N $Na_2B_4O_7{\cdot}10H_2O$ solution of pH = 8·44, at a scan rate of 1 mV/s. The intermetallics exhibited stable passive behaviour.

Table 1. Parameters determined from the potentiodynamic polarization curves for the carbon-alloyed iron aluminides.

Sample	b_a (V/dec.)	b_c (V/dec.)	E_{corr} (V)	i_{corr} (A/cm^2)	i_{crit} (A/cm^2)	E_{pass} (V)	i_{pass} (A/cm^2)	E_b (V)	Remarks
Fe–28·1Al–2·1C (pH = 8·4)	0·04	0·08	– 0·304	$2{\cdot}00 \times 10^{-7}$	–	–	$1{\cdot}3 \times 10^{-6}$	0·933	Stable passivity
Fe–28·1Al–2·1C (pH = 1·0)	0·20	0·26	– 0·537	$1{\cdot}54 \times 10^{-5}$	$6{\cdot}69 \times 10^{-3}$	0·36	$8{\cdot}3 \times 10^{-5}$	0·369	Active-passive
Fe–27·5Al–3·7C (pH = 8·4)	0·04	0·12	– 0·279	$3{\cdot}14 \times 10^{-7}$	–	–	$2{\cdot}8 \times 10^{-6}$	0·885	Stable passivity
Fe–27·5Al–3·7C (pH = 1·0)	0·24	0·27	– 0·573	$2{\cdot}44 \times 10^{-5}$	$9{\cdot}86 \times 10^{-3}$	0·41	$7{\cdot}2 \times 10^{-5}$	0·408	Active-passive

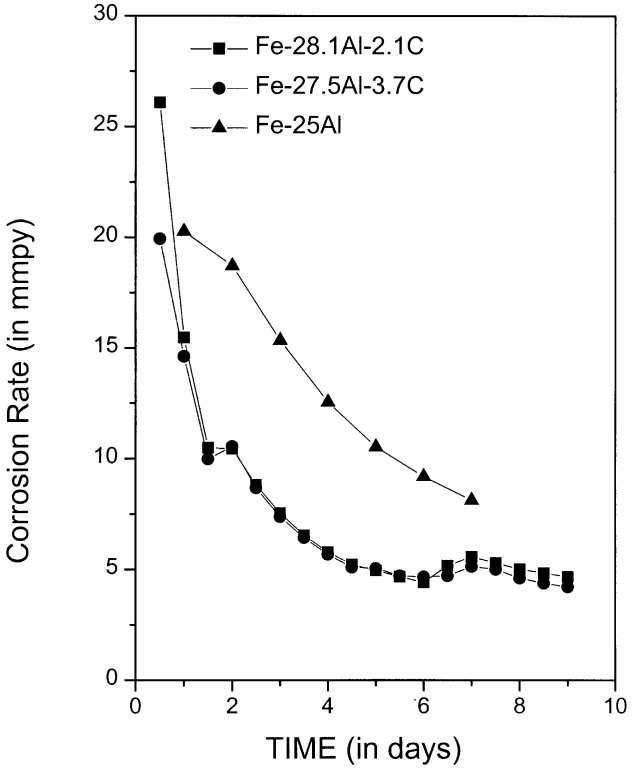

Figure 3. Corrosion rate as a function of time for the intermetallics in 0·05 mol/l H_2SO_4 solution. Data were obtained after 24 h intervals. The data for Fe–28Al is from Babu *et al* (2000).

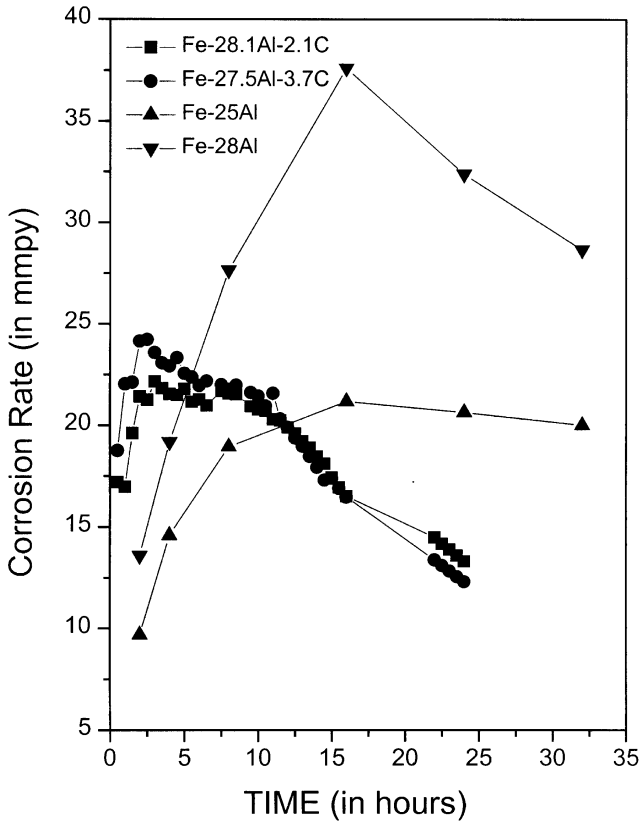

Figure 4. Corrosion rate as a function of time for the intermetallics in 0·05 mol/l H_2SO_4 solution. Data were obtained after 0·5 h intervals. The data for Fe–25Al and Fe–28Al is from Babu *et al* (2000).

medium) using the Tafel extrapolation method. The corrosion rate in millimeters per year (mmpy) was calculated from the corrosion current by the following relation (Jones 1992),

$$\text{Corrosion rate (in mmpy)} = C.E.\ I_{corr}/d.A,$$

where, C is the conversion factor ($= 3{\cdot}06 \times 10^5$) for obtaining rate in units of mmpy, E the equivalent weight of the intermetallic in g/mol, I_{corr} the corrosion current in amp, d the density of the intermetallic in g/cc and A the exposed cross section of the intermetallic in cm^2. For the carbon-alloyed intermetallics, the values of E and d were estimated as 21·7 g/mol and 6·72 g/cc, respectively. The cross sectional area exposed for the polarization experiment was 1 cm^2. The corrosion rates in the 0·05 mol/l H_2SO_4 solution thus obtained were 15·1 mmpy and 24·1 mmpy for Fe–28·1Al–2·1C and Fe–27·5Al–3·7C, respectively. The corrosion rates of the two alloys are similar and comparable to the corrosion rates determined using direct weight loss measurements by immersion testing, which will be discussed below.

3.2 *Immersion testing*

The weight loss data as a function of time was utilized to obtain the cumulative corrosion rate up to that point of

time. The corrosion rate as a function of time is presented in figure 3 for both the intermetallics. The rates of corrosion were high initially for both the intermetallics. Thereafter, the corrosion rate decreased and remained nearly constant in the last few days of the experiment. A similar behaviour was also observed for Fe–25Al (Babu *et al* 2000). In order to understand the high rate of corrosion in the initial stages, short-term immersion tests were carried out for a total duration of 24 h and the weight loss was measured after every 30 min. The results of these tests are presented in figure 4 for the intermetallics. The corrosion rate increased initially and after attaining a peak value at about 2 h, decreased continuously. Interestingly, the Fe–28Al specimen also exhibited a similar behaviour in that the corrosion rate was maximum after a certain period of immersion and then decreased with time. It is also important to note that the corrosion rates of both the carbon-alloyed intermetallics were comparable to those of Fe–25Al and Fe–28Al (Babu *et al* 2000).

The observed corrosion rate behaviour (i.e. high corrosion rate in the initial stages) could be due to selective dissolution. Selective dissolution implies either selective dissolution of one phase or selective dissolution from some specific locations in the material. The decrease in corrosion rate on continued immersion indicated that the intermetallics had attained an equilibrium surface layer. This can be explained based on the polarization behaviour. It is reasonable to propose that the critical current density for passivation would be attained due to the high rate of corrosion in the initial stages. The achievement of passivation is confirmed by the decrease in corrosion rate in the later stages, and also by the constant corrosion rate measured in the final stages (figure 3). In this regard, the presence of carbide–metal interfaces would accelerate the corrosion process and the critical current density would be attained in a shorter time than for the base intermetallic. This should result in shorter times to achieve the maximum in corrosion rate for the carbon-alloyed intermetallics when compared to the binary intermetallics. This has also been experimentally observed (figure 4). Another possible reason for the decrease in the corrosion rate with time is the decreasing corrodability of the solution with time. This seems unlikely in the present study as the solution (0·05 mol/l H_2SO_4) used for immersion testing was relatively strong.

3.3 *Microstructural features*

In order to gain further insights into the microstructural aspects of the corroding surfaces, independent immersion experiments were conducted and the corroded surfaces were observed in a JEOL JSM 840A scanning electron microscope. Both the carbon-alloyed intermetallics exhibited similar microstructural features—a uniform distribution of relatively large Fe_3AlC carbide precipitates in the matrix. A typical microstructure is provided in figure 5a.

The microstructures of both the samples were analyzed for obtaining information on the carbide particle distribution (the carbide particle size and its surface area per unit volume). For this purpose, five photographs of each sample were taken at different places at a magnification of 100×. The volume fraction of the carbide particles and

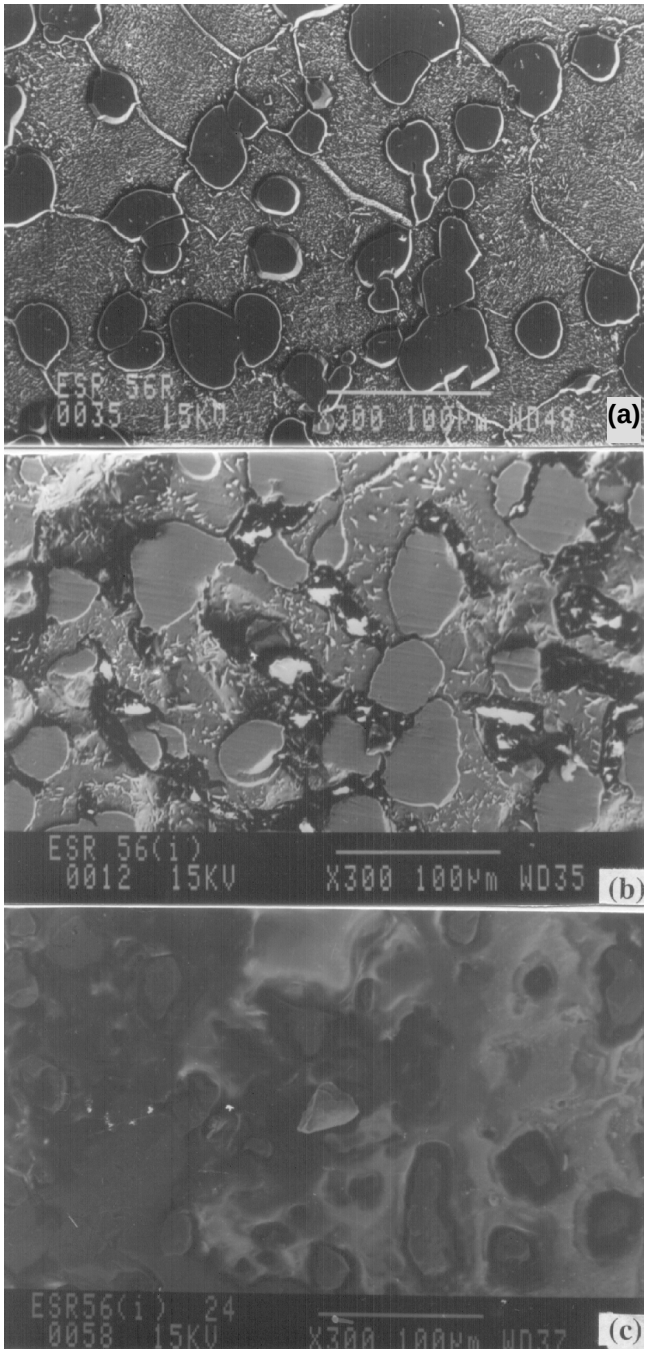

Figure 5. SEM micrograph of Fe–28·1Al–2·1C: **(a)** basic microstructure, **(b)** after immersion for 2 h and **(c)** after immersion for 24 h in 0·05 mol/l H_2SO_4 solution.

Table 2. Average diameter, volume fraction and surface area per unit volume of the carbide particles in the Fe–28·1Al–2·1C and Fe–27·5Al–3·7C alloys.

Sample	Average diameter (m) ($\times 10^6$)	Volume fraction	Surface area/vol. (m^2/m^3) ($\times 10^{-4}$)
Fe–28·1Al–2·1C	37	0·15	2·4
Fe–27·5Al–3·7C	42	0·25	3·5

their average mean diameter were estimated by image analysis (table 2). Assuming that the carbide particles were spherical in shape, the number of particles per unit volume was also calculated. With the known number of second phase carbide particles, the surface area of carbide particles per unit volume was estimated (table 2). It is noticed that the size of the spherical carbide particles was approximately the same in both the specimens. As the Fe–27·5Al–3·7C alloy contained higher carbon than the Fe–28·1Al–2·1C alloy, it possessed a higher carbide volume fraction and surface area per volume of the spherical carbide particles.

After 2 h of exposure in the 0·05 mol/l H_2SO_4 solution, the particle–matrix interfaces were the selective locations for corrosion (figure 5b). Deep corrosion pits at the carbide–matrix interfaces were observed in many locations after fairly long immersion times (figure 5c). Interestingly, the carbide particles were not corroded with respect to the matrix as a function of time. This is reasonable as carbon is a relatively noble material and the carbide (Fe_3AlC) contains a significant amount of carbon. The enhanced selective corrosion at the carbide–matrix interfaces could be because of the distance effect in galvanic corrosion (due to lower resistance near the interface). The matrix is expected to behave as the anode and carbide as the cathode in the local galvanic cells that form on the surface on immersion in the solution. Therefore, the matrix preferentially corrodes at the expense of the carbide, especially at the carbide–matrix interfaces. Interestingly, these selective dissolution sites can grow into deep pits with time, as has also been observed in the present study. Interestingly, the pits are potential sites for crack initiation by environmental degradation mechanism (stress corrosion cracking, hydrogen embrittlement, etc). It is therefore anticipated that the presence of carbides in the iron aluminide may not be beneficial for application of these intermetallics in immersion conditions, without the application of protective coatings.

4. Conclusions

The corrosion behaviour of two carbon-alloyed intermetallics of composition Fe–28·1Al–2·1C and Fe–27·5Al–3·7C has been studied. Potentiodynamic polarization studies indicated that the intermetallics exhibited active–passive behaviour in an acidic solution (0·05 mol/l H_2SO_4) of pH = 1, whereas they exhibited stable passivity in a buffer solution (0·15 N boric acid + 0·15 N $Na_2B_4O_7{\cdot}10H_2O$) of pH = 8·4. Corrosion rates were also obtained by immersion testing, wherein it was observed that both the intermetallics exhibited similar behaviour. The corrosion rates increased in the initial stage and acquired a maximum, after which they decreased. In the final stages, the corrosion rate remained almost constant. This behaviour has been related with the potentiodynamic polarization behaviour. Microstructural study of the surfaces indicated that the carbon-alloyed intermetallics were susceptible to galvanic corrosion due to the presence of the carbides in the intermetallic matrix.

Acknowledgements

The authors thank Dr D Banerjee and Dr R G Baligdad, DMRL, Hyderabad, for providing the specimens used in the present study.

References

Babu N, Balasubramaniam R and Ramesh Kumar A V 2000 (to be published)

Baligdad R G, Prakash U, Ramakrishna Rao V, Rao P K and Ballal N B 1994 *Iron & Steel Making* **21** 324

Baligdad R G, Prakash U, Radhakrishna A and Ramakrishna Rao V 1997a *Scr. Mater*. **36** 667

Baligdad R G, Prakash U, Radhakrishna A and Ramakrishna Rao V 1997b *Scr. Mater*. **36** 105

Jones D A 1992 *Principles and prevention of corrosion* (New York: Maxell Macmillan International)

Sen M and Balasubramaniam R 2000 *Scr. Mater.* (accepted)